Materials Science and Engineering C 45 (2014) 659–670

Contents lists available at ScienceDirect

Materials Science and Engineering C

journal homepage: www.elsevier.com/locate/msec

Biodegradable polymers for electrospinning: Towards biomedical applications

Dan Kai [a,1], Sing Shy Liow [a,1], Xian Jun Loh [a,b,c,*]

[a] Institute of Materials Research and Engineering (IMRE) Agency for Science, Technology and Research (A*STAR), 3 Research Link, Singapore 117602, Singapore
[b] Department of Materials Science and Engineering, National University of Singapore, 9 Engineering Drive 1, Singapore 117576, Singapore
[c] Singapore Eye Research Institute, 11 Third Hospital Avenue, Singapore 168751, Singapore

ARTICLE INFO

Article history:
Received 22 January 2014
Received in revised form 2 April 2014
Accepted 21 April 2014
Available online 28 April 2014

Keywords:
Electrospun nanofibers
Biodegradable polyesters
Tissue engineering
Drug delivery
Biosensors

ABSTRACT

Electrospinning has received much attention recently due to the growing interest in nano-technologies and the unique material properties. This review focuses on recent progress in applying electrospinning technique in production of biodegradable nanofibers to the emerging field of biomedical. It first introduces the basic theory and parameters of nanofibers fabrication, with focus on factors affecting the morphology and fiber diameter of biodegradable nanofibers. Next, commonly electrospun biodegradable nanofibers are discussed, and the comparison of the degradation rate of nanoscale materials with macroscale materials are highlighted. The article also assesses the recent advancement of biodegradable nanofibers in different biomedical applications, including tissue engineering, drug delivery, biosensor and immunoassay. Future perspectives of biodegradable nanofibers are discussed in the last section, which emphasizes on the innovation and development in electrospinning of hydrogels nanofibers, pore size control and scale-up productions.

1. Introduction

Electrospinning was first being introduced in early 1930s for fabrication of nanofibers as filter materials and textile yarns. Since 1990s, after Reneker et al. demonstrated the feasibility to produce electrospun nanofibers from many polymers, the number of publications about electrospinning has grown exponentially [1,2].

Electrospinning received much attention for biomedical applications mainly due to the growing interest in nano-technologies and the unique material properties. Electrospinning is an inexpensive and simple method to create nanoscale polymer fibers with diameter range from 3–5000 nm [3]. Nanofibers are suitable to mimic biological environment because they are in the same scale as biological molecules. In fact, nanomaterials like particles, fibrous morphologies or other complex forms, have shown improved interactions with cells, for example, selective endocytosis, adhesion and orientation [4–6]. In addition, large surface area to volume ratio (SVR) of these structures provides the nanofibrous mat high pore volumes with different pore sizes. These pores facilitate the loading of bioactive molecules and transportation of nutrients and waste. These outstanding properties enable the polymer nanofibers become an important class of biomaterial.

To date, over 100 types of natural and synthetic polymers were electrospun into nanofibers [7]. Popular materials includes: collagen, elastin, fibrinogen, alginates, polyesters, polyurethanes and their blends etc [8]. Nanofibers that are biodegradable and biocompatible have advantages in a few aspects: they metabolize into biocompatible degradation products in human body; therefore, second surgery for implant removal is unnecessary. Degradation profile of the nanofibers is tunable to match with the tissue regeneration time frame. Ideally nanofibers should degrade at the same pace as new tissue grows. Although degradation of polymers *in vitro* and *in vivo* is comprehensively studied, the degradation mechanisms of polymer nanofibers are still under-explored.

Based on relevant US patents filed in recent years, most of the applications nanofibers are in the field of biomedical prosthesis predominantly blood vessels and grafts. Specifically, biodegradable polymer nanofibers showed promising perspective in cosmetic, life science and tissue engineering scaffolds, in laboratory scale. More efforts are expected in future to scale-up these nanofibers into industrials scale.

In this review, we report brief theory and parameters of electrospinning process, types of biodegradable nanofibers and assess recent advancement of biodegradable nanofibers in different biomedical applications.

2. Fabrication of electrospun biodegradable nanofibers

2.1. Theory and parameters of electrospinning

Electrospinning is attractive thanks to the simplicity and inexpensive nature of setup. The basic setup for electrospinning is shown in

* Corresponding author at: Institute of Materials Research and Engineering (IMRE), 3 Research Link, Singapore 117602, Singapore.
E-mail addresses: lohxj@imre.a-star.edu.sg, XianJun_Loh@scholars.a-star.edu.sg (X.J. Loh).
[1] These authors contributed equally to this work.

http://dx.doi.org/10.1016/j.msec.2014.04.051
0928-4931/

Fig. 1(a) [9]. There are 3 elementary components to complete the process: a capillary tube as a reservoir for polymer solution, a high-voltage power supply, and a metallic collector. During the spinning process, high voltage (5–15 kV) is applied between a needle capillary end and a collector. The polymer solution is electrically charged. At the needle tip, the polymer solution deforms from a spherical pendant droplet to a conical shape, known as "Taylor cone". As the electric field is stronger than the surface tension of the polymer solution, the jet is ejected from the cone surface. As the jet travels, the solvent evaporates in the air, together with the stretching and acceleration of the polymer jet, leading to the extreme thin polymer fibers deposition on the collector [10]. Electrical bending instability occurs when the distance from the tip to collector is sufficiently long; in case of a short distance, the jet is typically straight. Fig. 1(b) shows the instability of polymer jet captured by high speed video [11]. Under the action of electric field, polymer jets experience the bending instability primarily due to mutual repulsion of the excess electric charges carried by electrospun jets.

The electrospinning process and the formation of polymer fibers are affected by many parameters. Spinnability, fiber diameters, fiber uniformity, fiber alignment, defects control (e.g. beads, junctions, and pores), and other properties are tunable by changing these parameters, (1) substrate-related parameters (polymer concentration, viscosity, molecular weight, surface tension); and (2) apparatus-related parameters (flow rate and electric field).

2.1.1. Substrate-related parameters

Most studies agreed that polymer viscosity the main determinants of fiber diameter and morphology. Increased viscosity due to high polymer molar mass or concentration can result in larger fiber diameters [2,12]. And also, beading is less likely to form, and more uniform fiber structures are observed [13,14].The relationship between polymer concentration and fiber diameter and morphology of biodegradable polymers including poly (DL-lactide-co-glycolide) (PLGA) (50:50), poly(DL-lactic acid) (PDLA), poly(L-lactide) (PLLA), gelatin, and dextran were reported in recent studies [9,13–17]. However, if the viscosity is too high, the flow of the polymer solution may be hindered and the droplet dries at the tip. On the other hand, if the viscosity is too low, fiber jet may break into droplets due to the lack of chain entanglement. For example, when the concentration of PLGA in (THF + DMF) was 0.10 g/mL or less, beads and droplets were obtained instead of nanofibers [9]. Ki et al. studied the gelatin nanofibers. In the range of polymer concentration of 8–12 wt. %, fiber diameter is exponentially increased with increasing polymer concentration. In other words, the change of fiber diameter vs. polymer concentration is nonliner. Uniform and beads-free gelatin fibers (76–169 nm) were obtained [16].

Polymer molar mass affects viscosity of polymer solution. Typically, low molar mass polymers lead to bead formation, while high molar mass polymers form fibers with larger diameters [10]. In addition, "electrospraying" happens instead of "electrospinning" when low molar mass polymers are used. Electrospraying results in small droplets due to instable jet formation. The spinnability of the polymer depends on the onset of chain entanglement between polymer chains, and it is varied for different polymers. For example, chitosan in acetic acid solution, with low molar mass of 30 kDa, it formed fragile fibers with many beads; with medium molar mass of 106 kDa, beads-free, uniform and continuous fibers (130 nm) were obtained [18].

The effect of surface tension of polymer solution on size or morphology of nanofibers is controversial. It depends on different polymer and solvent systems. Doshi and Reneker reported that by reducing surface tension of the polymer solution, beads-free fibers can be obtained. Zuo et al. reported the fiber morphologies of poly(hydroxybutyrate-co-valerate) (PHBV) in different solvent systems [19]. Smooth fibers were obtained when the surface tension of the solvent is lowered by adding alcohol. However, a lower surface tension is not always suitable for electrospinning. For example, acetone and dimethyacetamide (DMAc) have surface tension of 23.7 and 32.4 dyne/cm, respectively. Liu and Hsieh studied electrospinning of cellulose acetate and reported that using neither acetone nor DMAc alone can produce fiber free of beads. Only using a mixture of acetone and DMAc, beads-free fibers are obtained [20].

2.1.2. Apparatus-related parameters

Lower feeding rate (also known as flow rate of the polymer solution) leads to smaller diameter of the fibers [13]. On the other hand, high feeding rate results in more beads formation. Based on the results reported by Zuo et al., as the feeding rate increases, more solution is ejected from the needle tip [19]. The drying and evaporation of the solvent is less effective before the fiber reached the collector.

An increased in applied electric field typically resulted in reduced fiber diameter due to more stretching of the polymer solution. For PLGA, increase in voltage (from 0.375–1.0 kV/cm) resulted in significant reduction in fiber diameter, then the change of diameter was not significant when the voltage is further increased [9]. In addition, increasing applied voltage typically leads to more beads formation, for example in PDLA [14], chitosan [18] and gelatin [16]. However, for PHBV, higher voltage leads to formation of beads-free PHBV fibers [19].

2.2. Biodegradable polymers for electrospinning (synthetic/natural/blends)

The success of electrospun nanofibers that based on a wide range of biodegradable and biocompatible materials has been reported in recent reviews [21,22], including natural proteins such as collagen, gelatin, silk, chitosan and alginate; synthetic polymers such as polyglycolide (PGA), poly(ε-caprolactone) (PCL), PLA and their copolymers P(LLA-CL) and PLGA that have been approved by FDA for clinical use; and their blends [8]. Fig. 2 displays the biological, mechanical and physiochemical

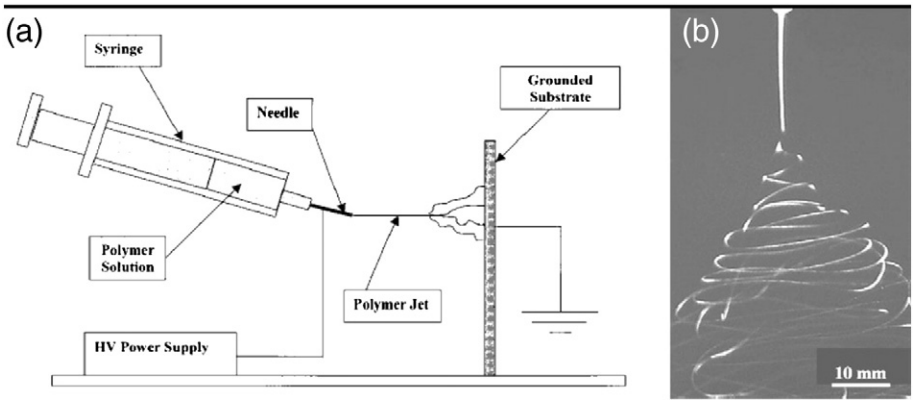

Fig. 1. (a) Schematic drawing of elementary setup for electrospinning. (Reprinted with permission from John Wiley and Sons [9]) (b) Typical bending instability of the jet during electrospinning captured by high speed video. (Reprinted with permission from Elsevier [11]).

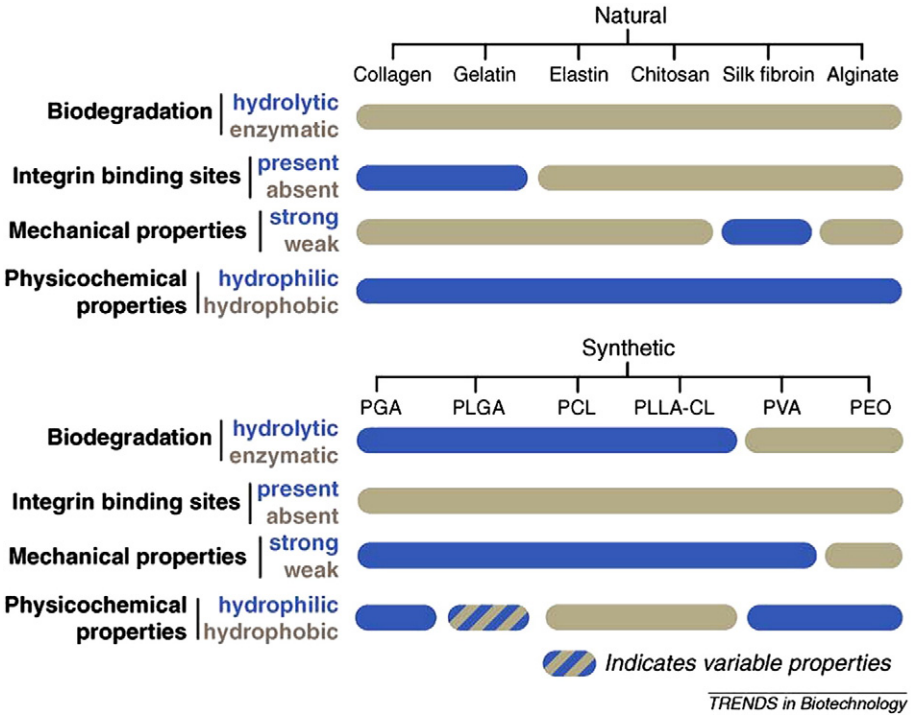

Fig. 2. Biological, mechanical and physiochemical properties of commonly studied biodegradable natural and synthetic polymer (reprinted with permission from Elsevier [8]).

properties of commonly studied biodegradable natural and synthetic polymers.

2.2.1. Macroscale vs. nanoscale, which one degrades faster?

It is reasonable that degradation behavior of nanofibers is different from their respective polymers in macroscales (e.g. polymer films, pellets). The structure of the nanofibers (e.g. 3D scaffolds, non-woven mat, membranes etc.) plays important role in determining the degradation profile of nanofibers. Compare nanofibrous scaffold with polymer films, electrospun nanofibrous scaffolds have higher surface area to volume ratio (SVR), and thus higher porosity. This facilitates the diffusion of degradation products, resulting in faster rate of degradation. Semicrystalline polymers nanofibers including PGA and PCL were reported showing this observation.

The degradation profile of PGA nanofibers was rapid without an induction period (first stage of degradation: water penetration or swelling without mass loss and morphology change) [23]. *In vitro* degradation showed 60 % weight loss in 20 days. PGA nanofibers degrade faster than microfibers and pellets because in PGA nanofibers, higher SVR allows higher water penetration into the highly crystalline matrix. Similar observation is reported for PCL nanofibers [23–25]. Thinner nanofibers showed faster diminishing trend in mechanical strength than nanofibers with larger diameters [26].

In contrary, the porosity of the electrospun nanofibrous scaffold reduces the autocatalytic effect resulted from accumulation of acidic degradation products, leading to slower degradation [27,28]. Amorphous poly (DL-lactide-co-glycolide) (PLGA) (50:50) polymer films samples (0.5 mm) degrades faster than their nanofibers (550 nm) because of autocatalysis effect within the polymer bulk [29].

2.3. Advanced electrospinning

2.3.1. Aligned fibers

Several studies have shown that the anisotropic structure and topography of aligned fibers not only resulted in anisotropic mechanical properties mimicking the ECM, but also shown improved interactions with cells, for example, selective endocytosis, adhesion and orientation [4–6]. The aligned fiber is formed when the fiber is collected on a rotating mandrel [30], by external electric field [10] or magnetic field [31]. Courtney et al. prepared aligned polyurethane-urea fibers using rotating mandrel [30]. Fig. 3 presents various degree of fiber alignment in correspond to the speed of the mandrel rotation. The aligned fibrous membrane exhibited stress-strain curves showing anisotropicity and modulus in the range of soft tissue, as illustrated in Fig. 4. Xie et al. demonstrated that radically aligned PCL fibers can induce faster cellular migration and population than random fibers [32]. The radically aligned fibers were fabricated by application of external electric field at the O-ring collector.

2.3.2. Core/shell fibers

Core/shell nanofibers show advantages in delivery of delicate drug in a sustained way and preventing decomposition or fast degradation of labile compounds. The core/shell nanofibers can be fabricated via coaxial electrospinning from two immiscible solutions. The basic setup of the coaxial electrospinning is essentially similar with the typical electrospinning except the introduction of the spinneret that consists of an inner capillary tube. Zhang et al. reported core/shell nanofibers made of gelatin-core and PCL-shell [33]. Their results showed that the overall diameters of the core/shell nanofibers are increased as the polymer concentration of the core material increases in the range of 7.5–15 w/v %.

3. Electrospun nanofibers in biomedical application

To date, the various applications of electrospun nanofibers have been widely expanded due to their advantages. For example, electrospun fibrous membranes possess high surface to volume ratio, high porosity and tunable physic-mechanical properties, as polymer solutions and process parameters can be easily adjusted to obtain desired fiber morphology and mechanical properties. In addition, a wide range of synthetic and natural polymers are able to be electrospun into nanofibers. From a biological perspective, the native extracellular matrix (ECM) of human tissues and organs is composed of a network of micro/nano-scaled protein and glycosaminoglycan fibers, which

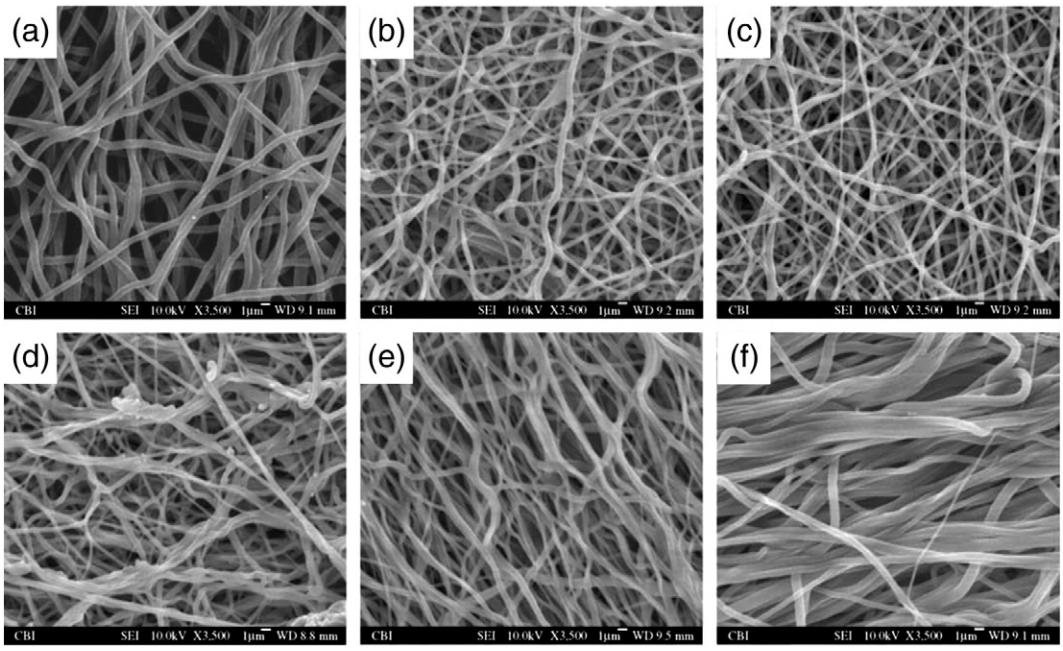

Fig. 3. Morphology changes of electrospun polyurethane-urea fibers as mandrel rotational velocity changes (a) random (b) 0.3 (c) 1.5 (e) 4.5 (f) 9.0 (g) 13.8 m/s (Reprinted with permission from Elsevier [30]).

provide support to resident cells and regulate cellular activities. With the similar fibrous architecture of native ECM, electrospun nanofibers have been broadly utilized in biomedical applications, such as tissue engineering, drug delivery, cosmetics and biosensors.

3.1. Tissue engineering

As an interdisciplinary technique, Tissue engineering (TE) uses three basic components (cells, scaffolds and biomolecules) to develop biofunctional substitutes for restore and maintenance of tissue function. However, it is still a big challenge to design an ideal scaffold that mimics the structure and biofunctions of the native ECM, and the capability of possessing the ECM-like nanofibrous structure is an essential consideration in rational design of TE scaffolds. Electrospun nanofibers, due to their nanofibrous structure and high surface area to volume ratio, have shown to favor the adhesion, proliferation and differentiation of various cells, and serve as promising scaffolds for tissue regeneration.

3.1.1. Nanofibers for skin tissue engineering

Electrospinning technique has greatly accelerated the development of innovative grafting scaffolds for skin TE. For wound healing application, the high porosity of electrospun nanofibers could provide more structural space for accommodation of the grafted cells, facilitate cell proliferation and migration and improve oxygen exchange, nutrient delivery and exudates extrusion. One the other hand, the small pore size of nanofibrous scaffolds is able to limit would wound infection and dehydration during wound healing. Additionally, the tunable mechanical properties of electrospun nanofibers could retain mechanical integrity between TE grafts and host tissue, and also prevent wound contraction during implanting.

Various natural and synthetic polymers have been electrospun into nanofibrous scaffolds for skin TE. Natural polymers, such as collagen, gelatin, silk, chitosan and fibrinogen, have been fabricated into nanofibers for wound healing, and cell culture results showed that those nanofibers could favor the attachment and proliferation of keratinocytes or fibroblasts [34–37]. Among all these natural polymers, collagen type I,

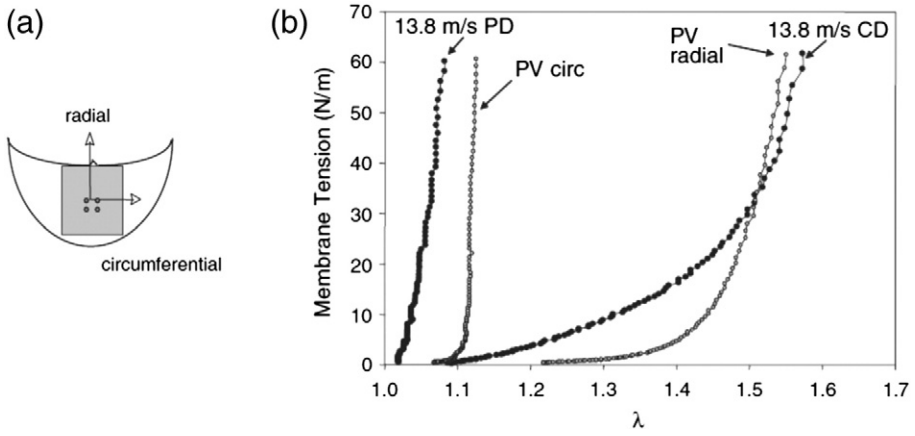

Fig. 4. (a) Schematic of the native pulmonary valve (PV) leaflet. (b) The biaxial tension vs. strain curves of the aligned fibrous membrane and the native PV. PD: preferred direction, CD: cross-preferred direction. (Reprinted with permission from Elsevier [30]).

composed of two α1 chains and one α2 chain, is a particular excellent candidate for skin TE scaffolds, because as the main component of human skin ECM, it forms a 3D network fibrillar structure (with fiber diameter of 50–500 nm) to modulate cell attachment, proliferation and differentiation in skin tissue [38]. Rho et al. electrospun collagen type I nanofibers with an average diameter of 460 nm and demonstrated that normal human keratinocytes exhibited improved cell adhesion and spreading rate on collagen type I nanofibers compared to other protein-coated nanofibers (fibronectin, bovine serum albumin and laminin) [39]. In addition, the animal study showed that early-state healing in the collagen nanofiber groups was promoted with the absence of surface tissue debris, prominent capillary and fibroblast proliferation. Vatankhah et al. developed cellulose acetate/gelatin electrospun nanofibers to mimic the composition of dermis ECM (a complex combination of proteins and polysaccharides), and they confirmed that electrospun cellulose acetate/gelatin 25:75 nanofibers showed distinct adherency features and high proliferation of human dermal fibroblasts [40]. However, the poor resistance of enzymatic degradation and weak mechanical properties are two major drawbacks of using natural polymers in TE. On the other hand, multiple biodegradable synthetic polymers, including PGA, PLA, PCL and their copolymers, are commonly used for skin and other TE because of their favorable mechanical and biodegradable properties. Kumber et al. fabricated PLGA electrospun nanofibers with different fiber diameters (150–6000 nm), and they found that PLGA nanofibers with fiber diameters in the range of 350–1100 nm showed improved cell proliferation and spreading of human skin fibroblasts and significantly upgraded the expression of collagen type III gene [41]. To investigate the relationship between the degradation properties of nanofibers and their efficacy for dermal regeneration, PLA and PLGA with different lactide/glycolide mole fractions (85:15, 75:25 and 50:50) were mixed and electrospun into nanofibers [42]. The *in vivo* study showed that PLLA nanofibers remained stable after 12 months of implantation whereas nanofibers of PLGA 85:15, 75:25 lost 50% of their original masses after 4 and 3 months, respectively. Among all the tested nanofibers, electrospun PLGA (85:15, 75:25) were demonstrated to be favorable biodegradable scaffolds for dermal replacement as beside supporting the growth of keratinocyte, fibroblast and endothelial cell, their degradation rate could match the healing rate in defected tissue (Fig. 5). However, the hydrophobic surface and the lack of cell-recognition signals limit the application of synthetic polymers. Recently,

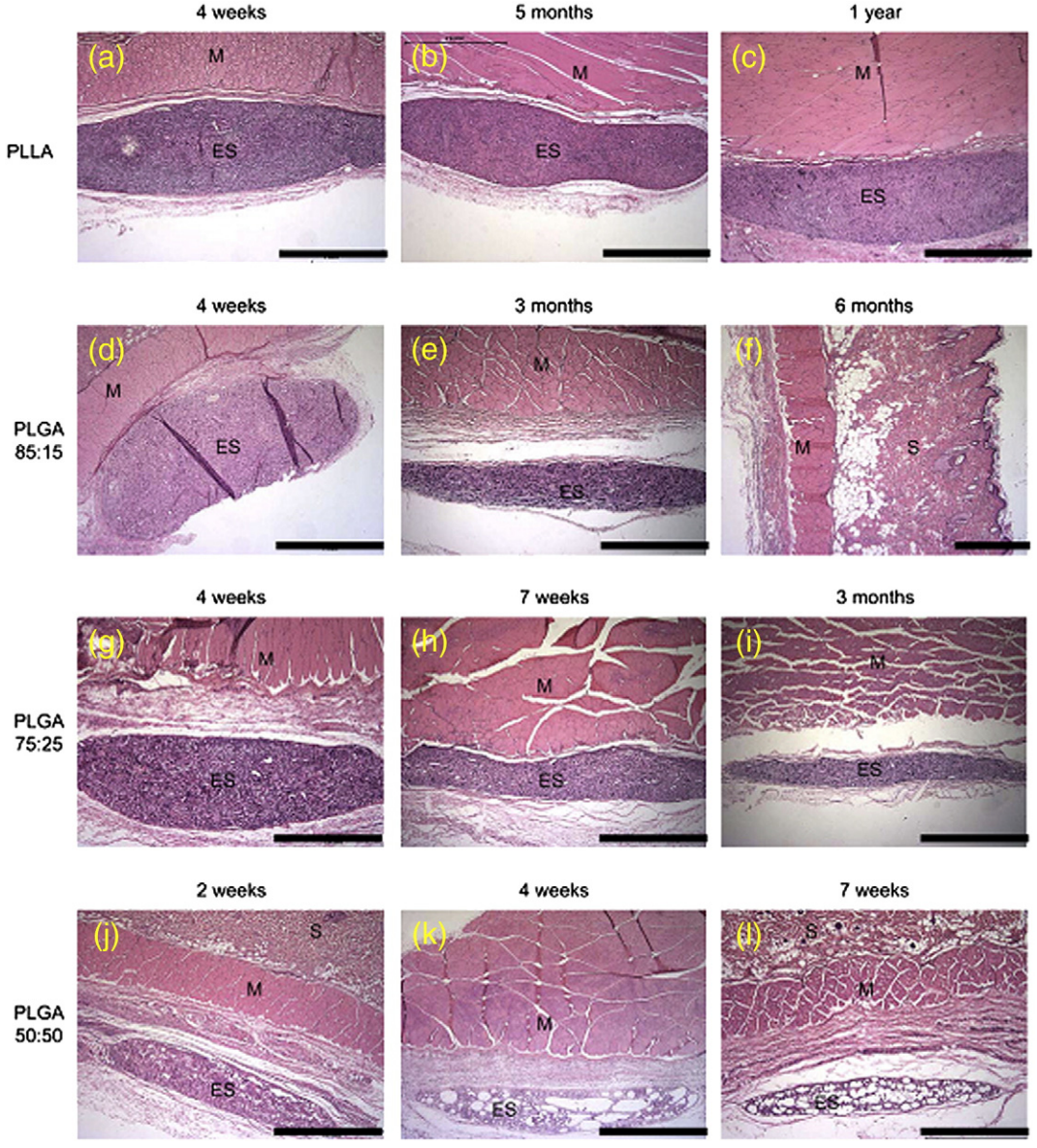

Fig. 5. H&E images of PLLA (a–c), PLGA 85:15 (D–F), PLGA 75:25 (g–l) following implantation into the flank of adult male Wistar rats at the time points indicated (2 weeks to 1 year). Implanted scaffold has been labelled as (ES), with underlying muscle (M) and skin (S). Scale bar = 1 mm (Reprinted with permission from Elsevier [42]).

more researches are focusing on composite nanofibrous scaffolds as they possess both the physical properties of synthetic polymers and bioactivity of natural polymers. For example, PLCL/collagen nanofibers were fabricated by electrospinning process, and compared to pure PLCL nanofibers, PLCL/collagen nanofibers not only increased the proliferation rate of human MSCs, but also promoted the epidermal differentiation of the stem cells [38]. Similarly, some other degradable composite nanofibers, such as PLGA/dextran, PCL/gelatin, PLCL/gelatin, PLCL/fibrinogen have been developed and fabricated for skin tissue engineering, and promising results were obtained [37,43–47].

As prevention of an infection during wound healing is crucial for skin regeneration, a wide range of anti-bacterial nanofibers incorporated with antibacterial agents (metallic, inorganic and organic)increasingly emerge and they show effective treatments for both the Gram-positive and the Gram-negative bacteria present during wound healing. Silver is the most commonly used metallic antibacterial agent, which displays a wide range of biocidal activity and a low bacterial resistance. In wound healing, silver shows the capability of reducing surface inflammation, increasing surface calcium and inducing epithelialization [48,49]. Jin et al. fabricated PLCL based antibacterial electrospun nanofibers by blending with different concentrations (0.25–0.75 wt.%) of silver nitrate ($AgNO_3$) for skin TE [50]. Results showed that the antibacterial activity of the nanofibers against Staphylococcus aureus and salmonella enterica was detected and the activity increased with the increasing concentration of silver nanoparticles in the nanofibers. Similarly, some other polymers, including PLA, PLGA, PVA, polysulfone, beta-cyclodextrin and polyurethane (PU), were also electrospun into nanofibers and blended or coated with silver nanoparticles to induce antibacterial properties [51–57]. However, in spite of its excellent antibacterial properties, sliver, like many other metals, could result in irritation and bind to DNA preventing to replication, causing cell death and hindering the healing processing. On the other hand, inorganic materials, such as titania, have been incorporated into polymeric electrospun nanofibers, which showed antimicrobial activity against multiple bacterial growth. Yan et al. prepared electrospun PU nanofibers with in-situ generated TiO_2 as a wound dressing, and the PU/TiO_2 nanofibers exhibited antibacterial efficiency against *Pseudomonas aeruginosa* and Staphylococcus aureus [58]. Later on, electrospun silk fibroin/TiO_2 nanofibers were fabricated and results showed that the nanofibers not only have good hemocompatibility and cytocompatibility, but also exhibited antibacterial activity against *Escherichia coli* under UV irradiation [59]. Moreover, carbon nanotubes were demonstrated to be highly cytotoxic to bacteria and kill microbes on contact. Schiffman has found that even at a low concentration (0.1 to 1 wt.%) of single-walled carbon nanotubes in electrospun polysulfone nanofibers, loss of bacteria (*Escherichia coli*) was observed [60]. In addition, inspired by nature, some native antibacterial agents, including shikonin, alkannin, fusidic acid, chitosan, lysostaphin and cinnamaldehyde, have been developed and incorporated into electrospun nanofiber to provide biocidal activity for wound healing [61–66].

3.1.2. Nanofibers for nerve tissue engineering

Other interesting application of electrospun nanofibers is for nerve regeneration. The aim of nerve TE is to develop effective neural guidance conduits for bridging gaps in damaged peripheral or central neurons, and the function of neural TE scaffolds should be directing axonal sprouting and promoting the diffusion of neurotrophic factors. Electrospun nanofibers are suitable materials for nerve TE as their structure not only mimics the neural fibrous ECM, but also provides substrate topographical guidance to direct neural cells growth[67].

It is reported that the properties of electrospun nanofibers (chemical components, diameter, orientation) could affect the proliferation, morphology and differentiation of neural cells. The presence of natural polymers in nanofibers is important for the growth of neural cells. Prabhakaran et al. demonstrated the advantage of collagen in neuronal differentiation of MSCs on electrospun nanofibers, and the results showed that human MSCs on PLCL/collagen nanofibers showed neuronal morphology, with multipolar elongations and expressed higher level of neuronal specific proteins such as neurofilament 200 and nestin, compared to pure PLCL nanofibers[68]. Beside collagen, laminin and gelatin also showed positive effects on neural growth and differentiation [69–71].As the direction of axon growth is a crucial consideration in neural regeneration, aligned nanofibers have been widely used in this field to promote neurite outgrowth and linkage to neighboring cells. Yang et al. found that aligned PLLA electrospun nanofibers would promote the elongation and neurite outgrowth of neonatal mouse cerebellum C17.2 stem cells parallel to the direction of aligned nanofibers [72].Similarly, Xie et al. reported that the aligned PCL nanofibers not only enhance the differentiation of embryonic stem cells (ESCs) into neural lineages but also direct the neurite outgrowth [73]. Furthermore, fiber diameter has been demonstrated as another factor to influence neural stem cells (NSCs) behavior. He et al. evaluated the effects of PLLA nanofibers with different fiber dimension on morphology of neonatal mouse cerebellum C17.2 stem cells, and results showed that wider cell spreading with decreasing fiber diameter, and the small diameter nanofibers (<500 nm) stimulated filopodia-like extensions of the cells, while the fibers with a relatively large diameter (>700 nm) resulted in a round morphology after 1 day of culture [74]. Christopherson et al. fabricated electrospun polyethersulfone (PES) fiber meshes with different fiber diameters (283 ± 45 nm, 749 ± 153 nm and 1452 ± 312 nm) to investigate the impact of fiber diameter on the differentiation of adult rat hippocampal-derived NSCs, and results showed that NSCs cultured on smaller diameter fibers differentiated preferentially into oligodendrocyte precursors, while the NSCs preferentially differentiated into neuronal precursors on the larger diametered (i.e. 749 nm) fibers (Fig. 6) [75].

Recently, the application of electrical stimulation (ES) in nerve TE has become an emerging approach to promote neurite growth and neural differentiation, and electrically conductive nanofibers have been developed as a crucial substrate for ES. Therefore, conductive polymers, such as polypyrrole (PPy), polyaniline (PANi), poly(3,4-ethylenedioxythiophene) (PEDOT) and even carbon nanotubes, have been incorporated into nanofibers during electrospinning. It is reported that conductive polymer-contained nanofibers could enhance the proliferation of nerve cells. Rat NSCson PLLA/PANi scaffolds showed higher proliferation than those on PLLA nanofibers after 8 days of cell culture [76]. Similarly, NSCs on PANi/PCL/gelatin nanofibers exhibited enhanced cell proliferation and neurite outgrowth compared to PCL/gelatin nanofibers under ES [77]. In another study, random and aligned PPy-coated PLGA nanofibers were fabricated and seed with rat PC12 cells [78]. Under the stimulation of 10 mV/cm potential, PC12 cells exhibited 40–50% longer neurites and 40–90% more neurite formation compared to those cells without ES. Moreover, cells on aligned conductive nanofibers showed longer neurites and more neurite-bearing cells than those on random nanofibers, indicating that both ES and topographical guidance affect neurite growth for nerve regeneration.

3.1.3. Nanofibers for cardiac tissue engineering

To date, heart disease has become the first leading cause of death all over the world, especially in developed countries, and cardiac TE gained great attention recently as it promises to revolutionize the treatment of patients with end-stage heart failure and provide new solutions to the serious problems of heart donor shortage [79,80]. Electrospun nanofibers have been considered high-attentive scaffolds for cardiac TE because their tunable mechanical properties and orientation of fibers are significant for myocardial regeneration [81]. Electrospun PCL nanofibers were fabricated and seeded with rat cardiomyocytes (CMs), and the cells attached on the scaffolds and started beating after 3 days, and the expression of cardiac-specific proteins such as α-myosin heavy chain, connexin43 and troponin I were detected after 14 days [82].Thick cardiac grafts were created by overlapping up to 5 layers of the cell-nanofiber membranes[83]. After 1 week of culture in vitro,

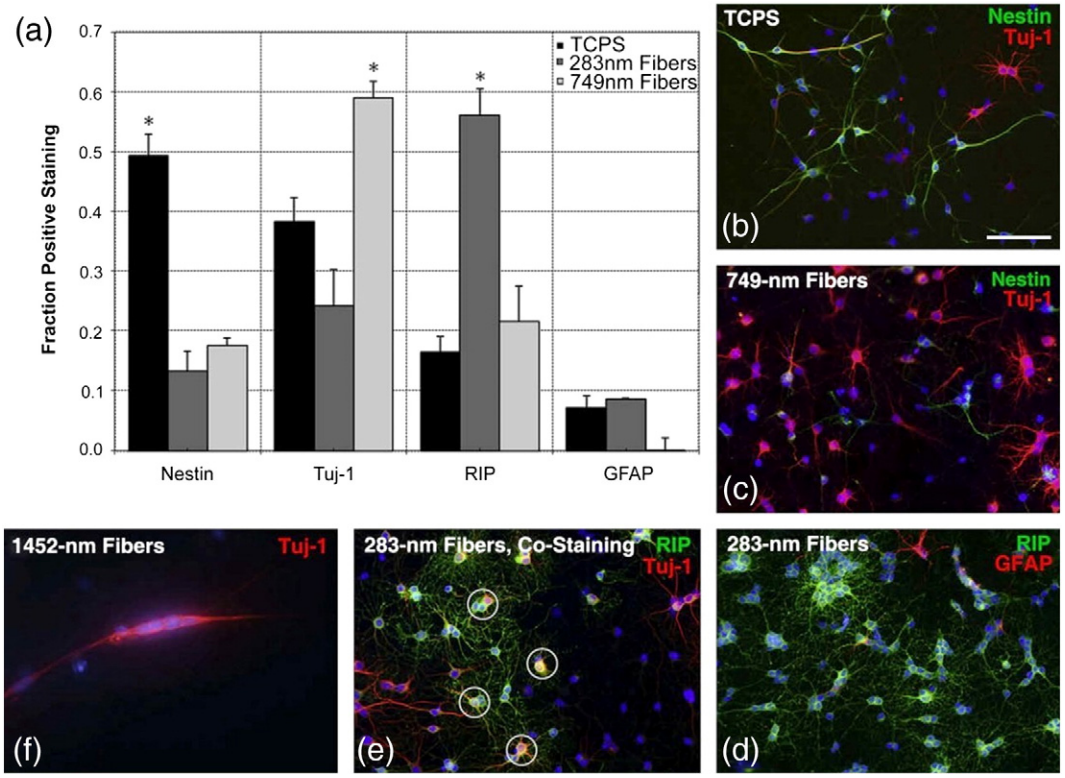

Fig. 6. Immunofluorescence analysis of rat NSCs cultured on TCP and nanofibers with different fiber diameters. Quantification of staining results is shown (a) with corresponding representative images of cells on each substrate (b–d). All images captured 200×, with scale bar = 100 μm. Circled cells on 283-nm fiber mesh are cells stained double positive for RIP and Tuj-1 (e). Example of statistically unquantifiable 1452-nm mesh is shown in (f) (Reprinted with permission from Elsevier [75]).

morphologic and electrical communication between the intimately adhered layers was established, and synchronized contraction was also observed. Stable and homogeneous PLGA/gelatin/elastin nanofibers were electrospun for cardiac TE, and the nanofibers were found to promote H9c2 rat cardiac myoblasts proliferation and assist MSCs to penetrate into the center of scaffolds [84]. The mechanical properties of cardiac scaffolds are crucial for the function of cardiac cells. PGS/fibrinogen core/shell nanofibers were fabricated with comparable stiffness of native myocardium, and Neonatal CMs cultured on nanofibers expressed high level of cardiac specific marker proteins, such as α-actinin, Troponin, β-myosin heavy chain and connexin 43 [85].

Cell alignment is also found in myocardial tissues and aligned ECM plays an important role in the behavior and function of cardiac cells in vivo, and therefore aligned nanofibers have been widely reported to direct the cell morphology and guide cell orientation in cardiac TE [86–88]. Aligned biodegradable non-woven PLGA nanofibrous membranes were electrospun to provide topographical cues for isotropic or anisotropic growth of neonatal rat CMs, and cell orientation and elongation were enhanced on aligned nanofibers [89]. Electrospun polymethylglutarimide (PMGI) nanofibrous meshes were fabricated to guide the orientation of CMs and aligned cell growth was guaranteed when the distance between fibers is below 30 μm [90].In another study, both electrospun PCL and PCL/gelatin nanofibers were fabricated and found to be able to guide the orientation of rabbit CMs [91]. Yet, greater cell alignment was observed on the aligned PCL/gelatin nanofibers compared to that on PCL nanofibers, indicating that both scaffold topography and constituents influence cell orientation. To mimic the cell alignment of myocardium and enhance cardiac differentiation, a tissue engineered cardiac graft was generated by simultaneously electrospinning elastic PU nanofibers and electrospraying MSCs [92]. By controlling the processing parameters, the obtained tissue constructs possessed the fibrous and anisotropic structure, and mechanical response similar to native myocardium. Enhanced cardiac differentiation was detected in the aligned cardiac nanofibrous graft by the higher expression of cardiac markers, such as GATA4, Nkx2.5 and MEF2C.

Some conductive nanofibers have also been used in cardiac TE. The co-electrospinning of PANi with gelatin was carried out to obtain conductive nanofibers and H9c2 rat cardiac myoblast cells were seeded to investigate their potential for cardiac TE [93]. Results showed that the concentration of PANi influenced the morphologies of cells seeded on them. PPy/PCL/gelatin conductive nanofibers were electrospun by blending different concentration of PPy into PCL/gelatin, and cell assay results showed that the proliferation of CMs on conductive nanofibers increased when the PPy concentration was 15%, whereas the proliferation rate reduced when PPy reached 30% [94].PLA/carbon nanotube nanofibers were electrospun as a conductive platform to direct MSCs differentiation towards a CM lineage under electrical stimulation [95]. Under ES, cells reoriented perpendicular to the direction of the electric field and adopted an elongated morphology. Moreover, an upgrade in a range of cardiac markers, such as cardiac myosin heavy chain, Nkx2.5, GATA-4, cardiac troponin T and connexin 43 were detected after 10 days.

3.1.4. Nanofibers for bone tissue engineering

Unlike soft tissues in our body, bone is a physically hard, rigid and strong connective tissue, which microscopically contains relatively small number of cells within abundant ECM in the form of collagen nanofibers and stiffening inorganic substrate, such as hydroxyapatite (HAp). Therefore, the unique bone ECM is an organic-inorganic nanofibrous composite, in which osteocytes are able to perform good functions and biological roles. To develop bone ECM mimicking scaffolds, electrospun composite nanofibers of degradable polymers and calcium phosphate are subject of substantial investigations for bone TE. Ngiam et al. fabricated mineralized polymeric nanofibrous composites by soaking electrospun PLLA or PLLA/collagen nanofibersin calcium chloride solution and disodium phosphate solution alternately, and they

noticed that bone-like nano-HAp was successfully deposited on both nanofibers, whereas the formation of nano-HAp on PLLA/collagen nanofibers was faster and more uniform than on PLLA nanofibers. Moreover, the nano-HAp deposited nanofibers showed enhanced capture efficacy of human fetal osteoblast cells within 20 min[96]. Later on, a novel bone scaffold was developed by simultaneous electrospraying of nano-HA on electrospun gelatin nanofibers, and the spin/spray gelatin/HA nanofibrous composite showed higher mechanical properties and promoted the cell proliferation, alkaline phosphatase (ALP) activity and mineralization of osteoblast cells compared to pure gelatin nanofibers [97].

Stem cell-based therapy for bone regeneration has aroused interest of many scientists, and among all stem cells, MSCs have been widely used in bone TE due to its easy availability, self-renewing ability and potential of osteogenic differentiation. Incorporation of nano-HAp into electrospun nanofibers has been also shown to promote cell adhesion and proliferation and even enhance osteogenic differentiation of MSCs. Lee et al. reported that human MSCs cultured on PLGA/HAp composite nanofibers exhibited enhanced ALP activity, upgraded expression of osteogenic genes and increased calcium mineralization compared to those on pure PLGA nanofibers [98]. Similarly, Peng et al. found that chitosan/HAp nanofibrous scaffolds not only supported better cell attachment and proliferation of mouse MSCs, but also promoted the osteogenic differentiation by up-regulating osteogenic gene expression, even in the absence of osteogenic supplementation [99]. Different concentrations (0–50%) of nano-HAp were blended into PCL to fabricate electrospun PCL/HAp nanofibers for bone TE, and results showed that MSCs on nanofibers showed increased cell proliferation rate and enhanced osteogenic differentiation capability (ALP activity and mineralization extent) with the increasing concentration of HAp in PCL nanofibers. Beside HAp, some other calcium salts, including beta-tricalcium phosphate, calcium carbonate, and even calcium phosphate cements, have been incorporated into polymeric nanofibers for bone TE, indicating that polymer/bioceramics nanofibrous composites are promising substrates for accelerating bone regeneration [100–102].

3.2. Drug delivery

The aim of designing a drug delivery system is to enable to control drug release towards alleviating medical conditions at a defined rate over a definite period [103]. Electrospun nanofibers have shown their advantages in the field of drug delivery due to their high surface area-volume ratio with interconnected pores in the fibers, which ensure better dissolution rate and high therapeutics take-up. Furthermore, the rate of drug release can be tailored for various applications by easily tuning relevant nanofiber properties, such as fiber diameter, porosity, and drug binding mechanisms [104]. To date, numbers of drugs and biomolecules, including genes, proteins and enzymes, have been successfully incorporated into electrospun nanofibers, mainly by two approaches: blending electrospinning and coaxial electrospinning [105]. Compared to blended nanofibers in which the polymer and biomolecules are mixed, the coaxial nanofibers encapsulate biomolecules inside of the polymers with a core-shell structure, leading to a reduced initial burst release and longer release period. PLCL nanofibers containing tetracycline hydrochloride (TCH) were fabricated by blending and coaxial electrospinning, and in vitro drug release study showed that 60–80% of loaded TCH was released within the first 5 h for the blended nanofibers, whereas the burst release from coaxial electrospun nanofibers was reduced to only 5–10% followed b stable and sustained release [106]. Later on, the same group reported that loading bone morphogenetic protein 2 (BMP-2) and dexamethasone into the core of PLCL/collagen nanofibers by coaxial electrospinning would lead to a controlled release rate of the two proteins compared to those from blended nanofibers [107]. Bovine serum albumin (BSA) as a model protein was incorporated into PCL nanofibers by blending and coaxial electrospinning. Coaxial nanofibers exhibited better sustained release profiles compared to blended nanofibers. Moreover, the addition of PEG into PCL nanofibers accelerated protein release and helped to preserve up to 5 % of the initial biological activity of the protein in the coaxial nanofibers [108].

Although electrospun nanofibers, especially coaxial nanofibers, show their advantages in drug delivery, several limitations still need to be addressed for their wider application. Initial burst release of drug from nanofibers is still one of major issues especially when the drug loading is high, as drug molecules tend to aggregate near the surface of fibers [109]. Recently, it was reported that the incorporation of superhydrophobic agent into nanofibers would be an effective way to reduce burst release at early stage and prolong the sustained release of drug. Highly hydrophobic electrospun PCL nanofibers loading with a model bioactive agent (SN-38) were fabricated by adding varying amounts (0–50%) of poly(glycerol monostearate-*co*-*ε*-caprolactone) (PGC-C18) as a hydrophobic polymer dopant [110]. Results showed that the release rate of SN-38 highly depending on the content of PGC-C18 and the apparent contact angle of the fiber, and the fibers with higher hydrophobicity resulted in slower release rate, as the air layers trapped within the hydropholic fibrous meshes would restrict water penetration. As a result, PCL nanofibers with high content of PGC-C18 (30 and 50%) exhibited less than 10% release over 60 days.

Besides control of initial burst release, the release of multiple drugs without interfering the release kinetics of each other is another issue to be solved. Therefore, study on nanofiber/particle electrospun composite for drug delivery is emerging fast, and different particle, including PLGA nanoparticles, alginate microspheres and chitosan microspheres were successfully incorporated into electrospun nanofibers [111–114]. With this technique, different drugs could be easily loaded into nanoparticles or nanofibers, especially hydrophobic drugs together with hydrophilic drugs. Xu et al. encapsulated BSA (as a hydrophilic model) into chitosan microspheres, dissolved benzoin (as a hydrophobic model drug) into PLLA solution, and fabricated PLLA fiber/ chitosan microsphere composites by electrospinning to investigate the dual release of these two drugs[114].Results showed that chitosan microspheres dispersed uniformly in the nanofibers, and the hydrophilic BSA had a short-term release while hydrophobic benzoin had a relative longer and sustained release. On the other hand, mesoporous silica nanoparticles (MSNs), due to their large specific surface area, tunable mesoporous structure and facile surface fictionalization, have emerged as promising drug delivery carriers and they have been incorporated into electrospun nanofibers as dual drug release system (Fig. 7) [115,116]. Song et al. developed dual drug-loaded PLGA/MSNs electrospun composites, where PLGA nanofibers were loaded with hydrophilic drug, fluorescein and MSNs were loaded with hydrophobic rhodamine B [117]. Results showed that separate and distinct profiles of two individual drugs were observed, indicating that there was no interaction between two drugs. Moreover, most of the fluorescein was fast released during the first 324 h, while rhodamine B exhibited a sustained release behavior. These studies have confirmed that the nanofiber/particle composite system is able to promote sustained and independent release of multiple drugs.

3.3. Biosensor and immunoassay

Biosensors, which are analytical devices for the detection of biological components (analytes), have been widely utilized for environmental, food and clinical application. As detection of gases and biological analytes normally is at low amount and concentration, sensitivity and limit-of-detection (LOD) play very important roles in the function of biosensors. Recently, researchers have recognized the advantage of increasing surface area of the detector substrate to increase the sensitivity and LOD of biosensors without increasing the amount of overall sample required, and therefore nanomaterials with extremely high surface area to volume ratio, which could increase the number of binding sites available for biological recognition element immobilization, are being

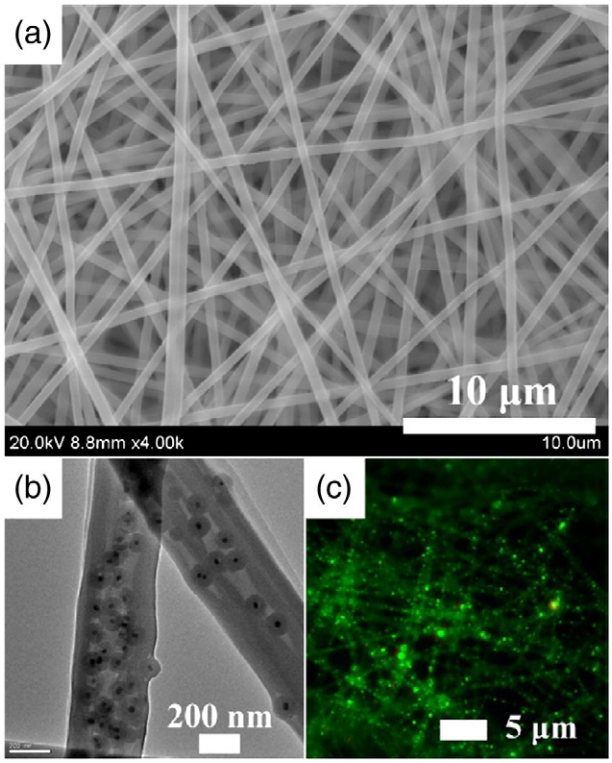

Fig. 7. SEM (a), TEM (b) and UC luminescence (c) images of PCL/gelatin/silica nanoparticles composite (Reprinted with permission from [115]. Copyright (2013) American Chemical Society).

integrated within analytical systems to allow for the detection of low concentrations of analytes without any complicated amplification processes[118,119]. Due to their unique characteristics, electrospun nanofibers have gained great attention in biosensor application. Besides their desirable large surface area to volume ratio, electrospun nanofibers can easily be functionalized through the incorporation of doping agents during spinning or through surface modification after spinning.

Fast glucose sensors with good sensitivity and selectivity are always highly demanded as glucose detection is remarkably vital to the patients suffering from diabetes. As glucose oxidase (GOD) is highly sensitive and selective to glucose and shows good stability in a large range of pH, this enzyme has been widely used to fabricate glucose biosensors. Recently, GOD has been successfully immobilized in/on various electrospun nanofibers for glucose detection. Ren et al. fabricated electrospun PVA/GOD nanofibers as a glucose biosensor, and chronoamperometric measurements showed that nanofibrous enzymatic electrodes exhibited a rapid response (1 s) and a higher response current (l A level) to glucose in the normal and diabetic level, and the linear response range (from 1 to 10 mM) and the LOD (0.05 mM) of the biosensor also meet the requirements of glucose detection in medical diagnosis[120]. Later on, a single ZnO nanofiber-based glucose biosensor was developed by functionalizing an individual electrospun ZnO nanofiber on a gold electrode with GOD by physical adsorption (Fig. 8) [121]. Electrochemical measurements revealed that the biosensor showed a high and reproducible sensitivity of 70.2 $\mu A cm^{-2}$ mM^{-1}within a response time of less than 4 s, as well as a linear range from 0.25 to 19 mM with a low LOD of 1 μM. Moreover, the biosensor exhibited a good anti-interference ability and favorable stability over relatively long-term storage (more than 4 months).Although numbers of new strategies have been explored to design advanced glucose enzyme sensors, insufficient stability due to the intrinsic nature of the enzyme limits the application of GOD based sensors. Therefore, recently more attentions have been paid on developments of non-enzymatic glucose sensing, and various carbon, metals (Au, Pt, Ni and Cu) and their oxides have been exploited as electrode materials to construct enzyme-free glucose sensors. For example, CuO nanofibers were prepared by electrospinning and subsequent thermal treatment processes for glucose non-enzymatic detection, and the biosensor showed a high sensitivity (431.3 μA cm^{-2} mM^{-1}), fast response (about1 s) and long-term stability [122]. Similarly, Co3O4 nanofiber-based glucose sensor was

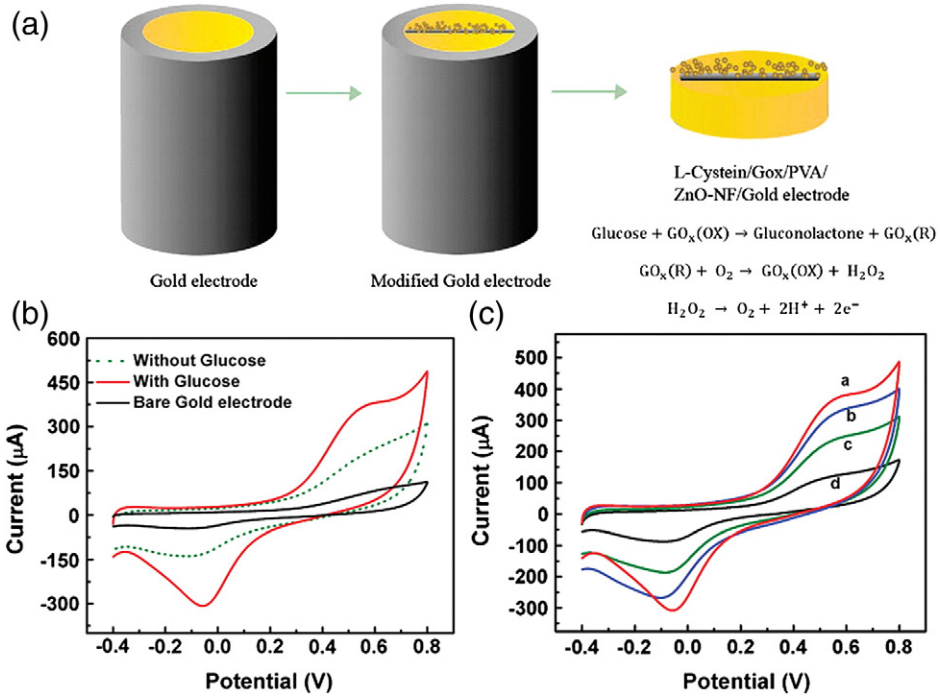

Fig. 8. a) Schematic diagram of the modified gold electrode and the mechanism of the glucose sensing on the modified electrode. (b) Cyclic voltammograms of the bare and modified gold electrode without and with 100 μM glucose in pH 7.0 PB solution. (c) Cyclic voltammograms of the biosensor in PB solution (pH 7.0) containing 100 μM glucose at a scan rate of (a) 100 mV, (b) 80, (c) 50, and (d) 20 mV s^{-1} (Reprinted with permission from [121]. Copyright (2010) American Chemical Society).

fabricated by electrospinning and subsequent calcination, and the biosensor exhibited a fast response time (less than 7 s), a high sensitivity of36.25 μA cm^{-2} mM^{-1}, good reproducibility and selectivity, and a detection limit of 0.97 μM (S/N = 3) [123]. In addition, its application in the detection of glucose inhuman blood serum sample showed agreed results with those obtained from commercial glucose meter, indicating that electrospun nanofibers show great potential applications in the development of biosensors for glucose detection.

Electrospun nanofibers incorporating a binder have been also used as a substrate for biosensor assay. In most immunoassay, streptavidin is utilized as substrate surface, which could be easily conjugated with a biotinylated biorecognition agent for the detection of specific target analytes, and recently, electrospun nanofibrous membranes, due to their large surface area, have been demonstrated as advanced substrates for biosensors based on biotin-streptavidin immobilization. Li et al. successfully incorporated biotin into PLA nanofibers through electrospinning and the streptavidin immobilized on PLA nanofibrous substrates could capture a biotinylated DNA probe [124]. On the other hand, Yang et al. electrospun poly(dimethylsiloxane) (PDMS)/poly(methyl methacrylate) (PMMA) nanofibers as substrates for protein microarrays, and the results of immunoassays demonstrated the superior performance of PDMS/PMMA nanofibers, where the LOD of nanofibrous substrates was 32 times lower than that on nitrocellulose membrane[125].

In research and clinical settings, Enzyme-linked immunosorbent assay (ELISA) is the current gold standard immunoassay due to its

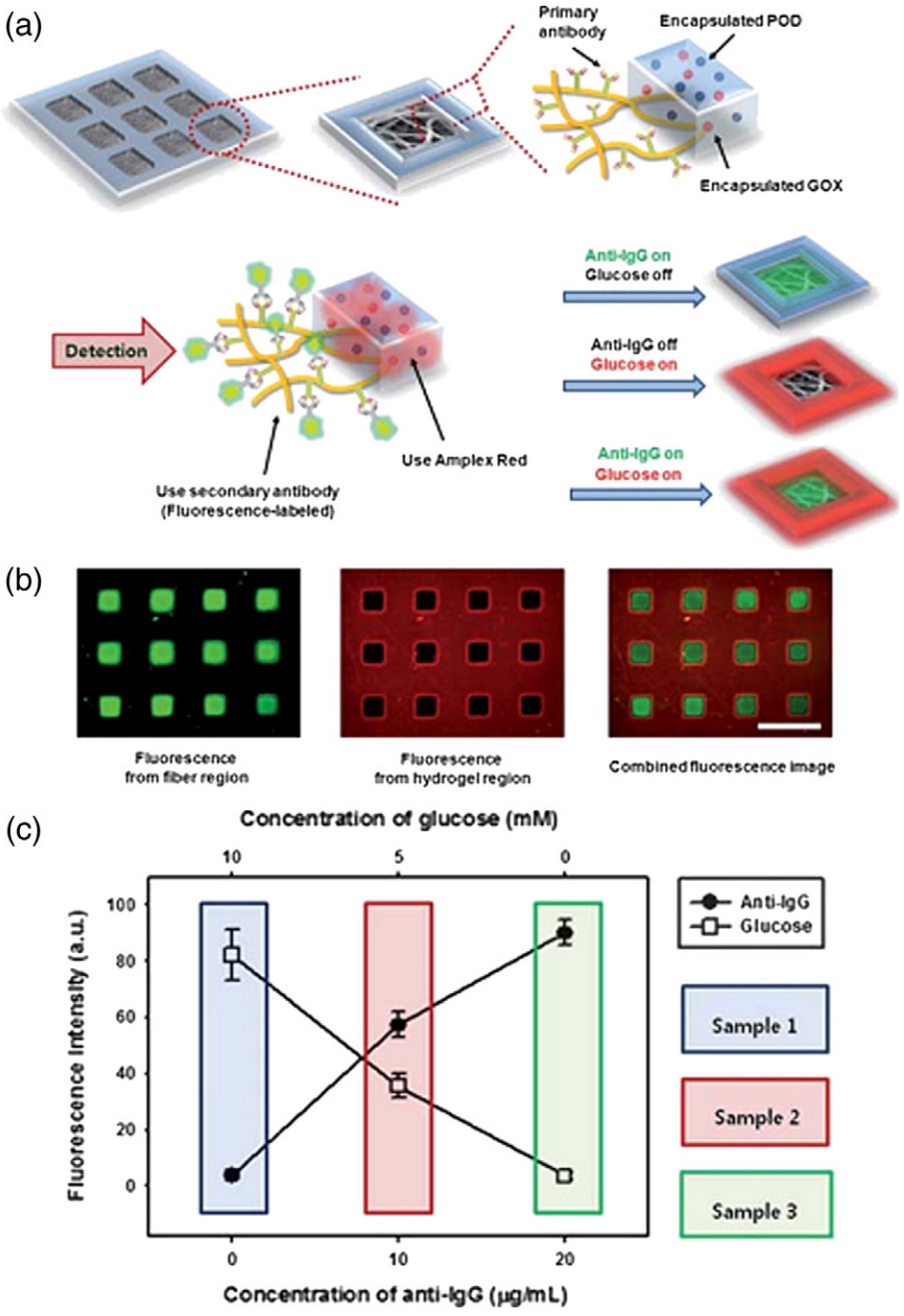

Fig. 9. Simultaneous analysis of immunoassay and enzyme-based assay using micropatterned PS/PSMA nanofibers. (a) Illustration of IgG-immobilized nanofibers that were micropatterned with enzyme-entrapped PEG hydrogel and detection logic, (b) fluorescence image of micropatterned PS/PSMA nanofibers that reacted with solution containing glucose, Amplex Red and FITC-labeled anti-IgG (scale bar = 500 mm), and (c) fluorescence intensity from the fiber and hydrogel region in the micropatterned nanofibers that reacted with three different samples (Reprinted with permission from Royal Society of Chemistry [128].

good sensitivity, and simple detection method. However, several drawbacks, such as long analysis time and low selectivity, limit its application. To overcome the weakness of ELISA, Tsou et al. prepared electrospun silica nanofiber membranes and investigated their use in ELISA[126]. It is reported that the LOD of nanofibrous ELISA was only 1.6 pM, 32 times lower compared to the conventional ELISA using polystyrene well plates, and the detection time was reduced to only 1 h. Similarly, electrospun PCL nanofibers conjugated with anti-HSA and HSA-FITC were prepared for immunoassay, and it was found that the folded and pressed PCL nanofibrous biosensor showed a linear detection range from 500 ng/mL down to 1 ng/mL, and a LOD of ~ 0.08 ng/mL, which is much lower than that of conventional nitrocellulose biosensor (~100 ng/mL)[127]. In addition, Lee et al. develop a new type of protein microarrays through a combination of electrospinning and hydrogel lithography (Fig. 9) [128]. IgG was selectively immobilized only within the nanofibrous region to create an IgG microarray, which showed a higher fluorescence signal and faster reaction rate compared to the planar substrates, while PEG hydrogels with the capability of encapsulating enzymes was used for protein micropatterns.

4. Perspectives and conclusion

As a traditional technology, electrospinning has shown its advantages in producing continuous micro/nanoscaled fibers with high surface area to volume ratio and porosity. Moreover, the properties of electrospun nanofibers (fiber diameter, mechanical property, surface property) can be easily modified by adjusting the electrospinning parameters according to different requirements. Therefore, desirable properties of electrospun nanofibers, including their mechanical behavior and biological characteristics, have gained lots of interests in biomedical application. On the other hand, to extend the application of electrospinning, electrospun nanofibers have been used together with other materials, such as hydrogels. The incorporation of nanofibers into hydrogels could improve the mechanical properties of the "nanocomposite hydrogel" system, by forming a complex fiber/gel architecture similar to the native ECM [129,130]. Furthermore, numbers of novel hydrogel polymers, including thermoresponsive polymers, pH-sensitive polymers, chemical crosslinked hydrogels and supramolecular polymers, have been synthesized and they showed great potential to fabricate into advanced biodegradable hydrogel nanofibers for multiple biomedical applications [131–138].

Despite of those advantages and success of electrospinning, there are still some critical imitations in this technology. The biggest challenge of electrospun nanofibers in biomedical engineering is difficulty in fabricating 3D scaffolds with macropores. The small pore size of electrospun nanofibers limits proper cellular infiltration into the fibers. Although some technologies, such as porogen-leaching, gas forming, low-temperature spinning, have been incorporated with electrospinning to increase the pore size in the resulted nanofibrous membranes. Another issue would be how to take this promising technology to production level, given its low production rate. While some pilot scale equipments, such as the Nanospider system from Elmarco, has been developed for large scale production of nanofibers, more study should be addressed on assessing the properties and characteristics of the fibers fabricated by the large scale equipment to ensure consistent fiber quality and evaluating the environmental issues associated with solvent/solution based electrospinning technology. Moreover, the mechanical properties, degradation rate and bioactivity of electrospun nanofibers need further investigations especially for biomedical applications. To summarize, electrospun nanofibers have proved to be a promising candidate in biomedical application and more research in this technology should be carried out for its entrance into the clinical application.

Supplementary data to this article can be found online at http://dx.doi.org/10.1016/j.msec.2014.04.051.

References

[1] D.H. Reneker, I. Chun, Nanotechnology 7 (1996) 216–223.
[2] J. Doshi, D.H. Reneker, J. Electrost. 35 (1995) 151–160.
[3] T. Subbiah, G.S. Bhat, R.W. Tock, S. Parameswaran, S.S. Ramkumar, J. Appl. Polym. Sci. 96 (2005) 557–569.
[4] W. Jiang, B.Y.S. Kim, J.T. Rutka, W.C.W. Chan, Nat. Nanotechnol. 3 (2008) 145–150.
[5] J. Gerardo-Nava, T. Fürmann, K. Klinkhammer, N. Seiler, J. Mey, D. Klee, M. Möller, P.D. Dalton, G.A. Brook, Nanomedicine 4 (2009) 11–30.
[6] D. Kai, G. Jin, M.P. Prabhakaran, S. Ramakrishna, Biotechnol. J. 8 (2013) 59–72.
[7] S. Agarwal, J.H. Wendorff, A. Greiner, Adv. Mater. 21 (2009) 3343–3351.
[8] J. Gunn, M. Zhang, Trends Biotechnol. 28 (2010) 189–197.
[9] D.S. Katti, K.W. Robinson, F.K. Ko, C.T. Laurencin, J. Biomed. Mater. Res. B Appl. Biomater. 70 (2004) 286–296.
[10] J.M. Deitzel, J.D. Kleinmeyer, J.K. Hirvonen, N.C. Beck Tan, Polymer 42 (2001) 8163–8170.
[11] T. Han, D.H. Reneker, A.L. Yarin, Polymer 48 (2007) 6064–6076.
[12] H. Fong, I. Chun, D.H. Reneker, Polymer 40 (1999) 4585–4592.
[13] H.S. Kim, K. Kim, H.J. Jin, I.J. Chin, Macromol. Symp. 224 (2005) 145–154.
[14] X.H. Zong, K. Kim, D.F. Fang, S.F. Ran, B.S. Hsiao, B. Chu, Polymer 43 (2002) 4403–4412.
[15] J. Zeng, H. Haoqing, A. Schaper, H. Wendorff Joachim, A. Greiner, Poly-L-lactide nanofibers by electrospinning-Influence of solution viscosity and electrical conductivity on fiber diameter and fiber morphology, vol. 3, e-Polymers, 2003, pp. 102–110.
[16] C.S. Ki, D.H. Baek, K.D. Gang, K.H. Lee, I.C. Um, Y.H. Park, Polymer 46 (2005) 5094–5102.
[17] H.L. Jiang, D.F. Fang, B.S. Hsiao, B. Chu, W.L. Chen, Biomacromolecules 5 (2004) 326–333.
[18] X. Geng, O.H. Kwon, J. Jang, Biomaterials 26 (2005) 5427–5432.
[19] W. Zuo, M. Zhu, W. Yang, H. Yu, Y. Chen, Y. Zhang, Polym. Eng. Sci. 45 (2005) 704–709.
[20] H.Q. Liu, Y.L. Hsieh, J. Polym. Sci. B Polym. Phys. 40 (2002) 2119–2129.
[21] N. Ashammakhi, A. Ndreu, A. Piras, L. Nikkola, T. Sindelar, H. Ylikauppila, A. Harlin, E. Chiellini, V. Hasirci, H. Redl, J. Nanosci. Nanotechnol. 6 (2006) 2693–2711.
[22] Y. Dong, S. Liao, M. Ngiam, C.K. Chan, S. Ramakrishna, Tissue Eng. B Rev. 15 (2009) 333–351.
[23] Y. You, B.M. Min, S.J. Lee, T.S. Lee, W.H. Park, J. Appl. Polym. Sci. 95 (2005) 193–200.
[24] K.E. Park, H.K. Kang, S.J. Lee, B.M. Min, W.H. Park, Biomacromolecules 7 (2006) 635–643.
[25] A.W.T. Shum, A.F.T. Mak, Polym. Degrad. Stab. 81 (2003) 141–149.
[26] N. Bölgen, Y.Z. Mencelo lu, K. Acatay, I. Vargel, E. Pişkin, J. Biomater. Sci. Polym. Ed. 16 (2005) 1537–1555.
[27] M. Therin, P. Christel, S. Li, H. Garreau, M. Vert, Biomaterials 13 (1992) 594–600.
[28] K.A. Athanasiou, J.P. Schmitz, C.M. Agrawal, Tissue Eng. 4 (1998) 53–63.
[29] H.J. Shin, C.H. Lee, I.H. Cho, Y.J. Kim, Y.J. Lee, I.A. Kim, K.D. Park, N. Yui, J.W. Shin, J. Biomater. Sci. Polym. Ed. 17 (2006) 103–119.
[30] T. Courtney, M.S. Sacks, J. Stankus, J. Guan, W.R. Wagner, Biomaterials 27 (2006) 3631–3638.
[31] Y. Liu, X. Zhang, Y. Xia, H. Yang, Adv. Mater. 22 (2010) 2454–2457.
[32] J. Xie, M.R. MacEwan, W.Z. Ray, W. Liu, D.Y. Siewe, Y. Xia, ACS Nano 4 (2010) 5027–5036.
[33] Y. Zhang, Z.M. Huang, X. Xu, C.T. Lim, S. Ramakrishna, Chem. Mater. 16 (2004) 3406–3409.
[34] J.P. Chen, G.Y. Chang, J.K. Chen, Colloids Surf. A Physicochem. Eng. Asp. 313 (2008) 183–188.
[35] M. Skotak, S. Noriega, G. Larsen, A. Subramanian, J. Biomed. Mater. Res. A 95A (2010) 828–836.
[36] A. Schneider, X.Y. Wang, D.L. Kaplan, J.A. Garlick, C. Egles, Acta Biomater. 5 (2009) 2570–2578.
[37] C. He, X. Xu, F. Zhang, L. Cao, W. Feng, H. Wang, X. Mo, J. Biomed. Mater. Res. A 97A (2011) 339–347.
[38] G.R. Jin, M.P. Prabhakaran, S. Ramakrishna, Acta Biomater. 7 (2011) 3113–3122.
[39] K.S. Rho, L. Jeong, G. Lee, B.M. Seo, Y.J. Park, S.D. Hong, S. Roh, J.J. Cho, W.H. Park, B.M. Min, Biomaterials 27 (2006) 1452–1461.
[40] E. Vatankhah, M.P. Prabhakaran, G.R. Jin, L.G. Mobarakeh, S. Ramakrishna, J. Biomater. Appl. 28 (2014) 909–921.
[41] S.G. Kumbar, S.P. Nukavarapu, R. James, L.S. Nair, C.T. Laurencin, Biomaterials 29 (2008) 4100–4107.
[42] K.A. Blackwood, R. McKean, I. Canton, C.O. Freeman, K.L. Franklin, D. Cole, I. Brook, P. Farthing, S. Rimmer, J.W. Haycock, A.J. Ryan, S. MacNeil, Biomaterials 29 (2008) 3091–3104.
[43] N.T. Dai, M.R. Williamson, N. Khammo, E.F. Adams, A.G.A. Coombes, Biomaterials 25 (2004) 4263–4271.
[44] G.R. Jin, M.P. Prabhakaran, D. Kai, S.K. Annamalai, K.D. Arunachalam, S. Ramakrishna, Biomaterials 34 (2013) 724–734.
[45] E. Chong, T. Phan, I. Lim, Y. Zhang, B. Bay, S. Ramakrishna, C. Lim, Acta Biomater. 3 (2007) 321–330.
[46] H. Pan, H.L. Jiang, W.L. Chen, Biomaterials 27 (2006) 3209–3220.
[47] S.I. Jeong, A.Y. Lee, Y.M. Lee, H. Shin, J. Biomater. Sci. Polym. Ed. 19 (2008) 339–357.
[48] H. Penchev, D. Paneva, N. Manolova, I. Rashkov, Macromol. Biosci. 9 (2009) 884–894.
[49] K.A. Rieger, N.P. Birch, J.D. Schiffman, J. Mater. Chem.B 1 (2013) 4531–4541.
[50] G.R. Jin, M.P. Prabhakaran, B.P. Nadappuram, G. Singh, D. Kai, S. Ramakrishna, J. Biomater. Sci. Polym. Ed. 23 (2012) 2337–2352.

[51] K.A. Khalil, H. Fouad, T. Elsarnagawy, F.N. Almajhdi, Int. J. Electrochem. Sci. 8 (2013) 3483–3493.
[52] R. Nirmala, D. Kalpana, R. Navamathavan, Y.S. Lee, H.Y. Kim, J. Nanosci. Nanotechnol. 13 (2013) 4686–4693.
[53] T.T.T. Nguyen, B. Tae, J.S. Park, J. Mater. Sci. 46 (2011) 6528–6537.
[54] H.H. Chae, B.H. Kim, K.S. Yang, J.I. Rheed, Synth. Met. 161 (2011) 2124–2128.
[55] Z.C. Xing, W.P. Chae, M.W. Huh, L.S. Park, S.Y. Park, G. Kwak, K.B. Yoon, I.K. Kang, J. Nanosci. Nanotechnol. 11 (2011) 61–65.
[56] L.R. Lakshman, K.T. Shalumon, S.V. Nair, R. Jayakumar, J. Macromol. Sci.A Pure Appl. Chem. 47 (2010) 1012–1018.
[57] J.D. Schiffman, Y. Wang, E.P. Giannelis, M. Elimelech, Langmuir 27 (2011) 13159–13164.
[58] L.D. Yan, S.X. Si, Y. Chen, T. Yuan, H.J. Fan, Y.Y. Yao, Q.Y. Zhang, Fibers Polym. 12 (2011) 207–213.
[59] W.C. Jao, M.C. Yang, C.H. Lin, C.C. Hsu, Polym. Adv. Technol. 23 (2012) 1066–1076.
[60] J.D. Schiffman, M. Elimelech, ACS Appl. Mater. Interfaces 3 (2011) 462–468.
[61] G. Dogan, F. Ozyildiz, G. Basal, A. Uzel, Int. Polym. Process. 28 (2013) 143–150.
[62] S.S. Said, O.M. El-Halfawy, H.M. El-Gowelli, A.K. Aloufy, N.A. Boraei, L.K. El-Khordagui, Eur. J. Pharm. Biopharm. 80 (2012) 85–94.
[63] J. Han, T.X. Chen, C.J. Branford-White, L.M. Zhu, Int. J. Pharm. 382 (2009) 215–221.
[64] K.N. Kontogiannopoulos, A.N. Assimopoulou, I. Tsivintzelis, C. Panayiotou, V.P. Papageorgiou, Int. J. Pharm. 409 (2011) 216–228.
[65] J.J. Miao, R.C. Pangule, E.E. Paskaleva, E.E. Hwang, R.S. Kane, R.J. Linhardt, J.S. Dordick, Biomaterials 32 (2011) 9557–9567.
[66] K.R. Zodrow, J.D. Schiffman, M. Elimelech, Langmuir 28 (2012) 13993–13999.
[67] R.L. Dahlin, F.K. Kasper, A.G. Mikos, Tissue Eng. B Rev. 17 (2011) 349–364.
[68] M. Prabhakaran, J. Venugopal, S. Ramakrishna, Biomaterials 30 (2009) 4996–5003.
[69] L. Ghasemi-Mobarakeh, M. Prabhakaran, M. Morshed, M. Nasr-Esfahani, S. Ramakrishna, Biomaterials 29 (2008) 4532–4539.
[70] N.E. Zander, J.A. Orlicki, A.M. Rawlett, T.P. Beebe, Biointerphases 5 (2010) 149–158.
[71] R.A. Neal, S.S. Tholpady, P.L. Foley, N. Swami, R.C. Ogle, E.A. Botchwey, J. Biomed. Mater. Res. A 100A (2012) 406–423.
[72] F. Yang, R. Murugan, S. Wang, S. Ramakrishna, Biomaterials 26 (2005) 2603–2610.
[73] J. Xie, S.M. Willerth, X. Li, M.R. Macewan, A. Rader, S.E. Sakiyama-Elbert, Y. Xia, Biomaterials 30 (2009) 354–362.
[74] L.M. He, S.S. Liao, D.P. Quan, K. Ma, C. Chan, S. Ramakrishna, J.A. Lu, Acta Biomater. 6 (2010) 2960–2969.
[75] G.T. Christopherson, H. Song, H.-Q. Mao, Biomaterials 30 (2009) 556–564.
[76] M.P. Prabhakaran, L. Ghasemi-Mobarakeh, G.R. Jin, S. Ramakrishna, J. Biosci. Bioeng. 112 (2011) 501–507.
[77] L.G. Ghasemi-Mobarakeh, M.P. Prabhakaran, M. Morshed, M.H. Nasr-Esfahani, S. Ramakrishna, Tissue Eng. A 15 (2009) 3605–3619.
[78] J.Y. Lee, C.A. Bashur, A.S. Goldstein, C.E. Schmidt, Biomaterials 30 (2009) 4325–4335.
[79] G. Vunjak-Novakovic, N. Tandon, A. Godier, R. Maidhof, A. Marsano, T.P. Martens, M. Radisic, Tissue Eng. B Rev. (2009) 140–568.
[80] Q.Z. Chen, S.E. Harding, N.N. Ali, A.R. Lyon, A.R. Boccaccini, Mater. Sci. Eng. R. Rep. 59 (2008) 1–37.
[81] F. Wang, J.J. Guan, Adv. Drug Deliv. Rev. 62 (2010) 784–797.
[82] M. Shin, O. Ishii, T. Sueda, J.P. Vacanti, Biomaterials 25 (2004) 3717–3723.
[83] O. Ishii, M. Shin, T. Sueda, J. Vacanti, J. Thorac. Cardiovasc. Surg. 130 (2005) 1358–1363.
[84] M. Li, M.J. Mondrinos, X. Chen, M.R. Gandhi, F.K. Ko, P.I. Lelkes, J. Biomed. Mater. Res. A 79 (2006) 963–973.
[85] R. Ravichandran, J.R. Venugopal, S. Sundarrajan, S. Mukherjee, R. Sridhar, S. Ramakrishna, Int. J. Cardiol. 167 (2013) 1461–1468.
[86] S.M. Factor, T.F. Robinson, Lab. Investig. 58 (1988) 150–156.
[87] Z. Ma, W. He, T. Yong, S. Ramakrishna, Tissue Eng. 11 (2005) 1149–1158.
[88] E. Kijeńska, M.P. Prabhakaran, W. Swieszkowski, K.J. Kurzydlowski, S. Ramakrishna, J. Biomed. Mater. Res. B Appl. Biomater. 100B (2012) 1093–1102.
[89] X. Zong, H. Bien, C. Chung, L. Yin, D. Fang, B. Hsiao, B. Chu, E. Entcheva, Biomaterials 26 (2005) 5330–5338.
[90] Y. Orlova, N. Magome, L. Liu, Y. Chen, K. Agladze, Biomaterials 32 (2011) 5615–5624.
[91] D. Kai, M.P. Prabhakaran, G.R. Jin, S. Ramakrishna, J. Biomed. Mater. Res. B Appl. Biomater. 98B (2011) 379–386.
[92] J.J. Guan, F. Wang, Z.Q. Li, J. Chen, X.L. Guo, J. Liao, N.I. Moldovan, Biomaterials 32 (2011) 5568–5580.
[93] M. Li, Y. Guo, Y. Wei, A.G. MacDiarmid, P.I. Lelkes, Biomaterials 27 (2006) 2705–2715.
[94] D. Kai, M.P. Prabhakaran, G.R. Jin, S. Ramakrishna, J. Biomed. Mater. Res. A 99A (2011) 376–385.
[95] E. Mooney, J.N. Mackle, D.J.P. Blond, E. O'Cearbhaill, G. Shaw, W.J. Blau, F.P. Barry, V. Barron, J.M. Murphy, Biomaterials 33 (2012) 6132–6139.
[96] M. Ngiam, S. Liao, A.J. Patil, Z. Cheng, F. Yang, M.J. Gubler, S. Ramakrishna, C.K. Chan, Tissue Eng. A 15 (2009) 535–546.
[97] L. Francis, J. Venugopal, M.P. Prabhakaran, V. Thavasi, E. Marsano, S. Ramakrishna, Acta Biomater. 6 (2010) 4100–4109.
[98] J.H. Lee, N.G. Rim, H.S. Jung, H. Shin, Macromol. Biosci. 10 (2010) 173–182.
[99] H.J. Peng, Z. Yin, H.H. Liu, X. Chen, B. Feng, H.H. Yuan, B. Su, H.W. Ouyang, Y.Z. Zhang, Nanotechnology 23 (2012) 10.
[100] K. Fujihara, M. Kotaki, S. Ramakrishna, Biomaterials 26 (2005) 4139–4147.
[101] H.S. Fan, X.T. Wen, Y.F. Tan, R. Wang, H.D. Cao, X.D. Zhang, Compare of electrospinning PLA and PLA/beta-TCP scaffold in vitro, in: Z.Y. Zhong, H. Saka, T. H. Kim, E.A. Holm, Y.F. Han, X.S. Xie (Eds.), Pricm 5: The Fifth Pacific Rim International Conference on Advanced Materials and Processing, Pts 1-5, vol. 475–479, Trans Tech Publications Ltd, Zurich-Uetikon, 2005, pp. 2379–2382.
[102] C. Bao, W. Chen, M.D. Weir, W. Thein-Han, H.H.K. Xu, Acta Biomater. 7 (2011) 4037–4044.
[103] N. Bhardwaj, S.C. Kundu, Biotechnol. Adv. 28 (2010) 325–347.
[104] V. Leung, F. Ko, Polym. Adv. Technol. 22 (2011) 350–365.
[105] A.K. Moghe, B.S. Gupta, Polymer Reviews 48 (2008) 353–377.
[106] Y. Su, X.Q. Li, H.S. Wang, C.L. He, X.M. Mo, J. Mater. Sci: Mater. Med. 20 (2009) 2285–2294.
[107] Y. Su, Q.Q. Su, W. Liu, M. Lim, J.R. Venugopal, X.M. Mo, S. Ramakrishna, S.S. Al-Deyab, M. El-Newehy, Acta Biomater. 8 (2012) 763–771.
[108] W. Ji, F. Yang, J. van den Beucken, Z.A. Bian, M.W. Fan, Z. Chen, J.A. Jansen, Acta Biomater. 6 (2010) 4199–4207.
[109] C.B. Weldon, J.H. Tsui, S.A. Shankarappa, V.T. Nguyen, M.L. Ma, D.G. Anderson, D.S. Kohane, J. Control. Release 161 (2012) 903–909.
[110] S.T. Yohe, Y.L. Colson, M.W. Grinstaff, J. Am. Chem. Soc. 134 (2012) 2016–2019.
[111] M. Beck-Broichsitter, M. Thieme, J. Nguyen, T. Schmehl, T. Gessler, W. Seeger, S. Agarwal, A. Greiner, T. Kissel, Macromol. Biosci. 10 (2010) 1527–1535.
[112] C. Kriegel, K.A. Kit, D.J. McClements, J. Weiss, Langmuir 25 (2009) 1154–1161.
[113] H.X. Qi, P. Hu, J. Xu, A.J. Wang, Biomacromolecules 7 (2006) 2327–2330.
[114] J.Q. Xu, Y.P. Jiao, X.H. Shao, C.R. Zhou, Mater. Lett. 65 (2011) 2800–2803.
[115] K.X. Qiu, C.L. He, W. Feng, W.Z. Wang, X.J. Zhou, Z.Q. Yin, L. Chen, H.S. Wang, X.M. Mo, J. Mater. Chem. B 1 (2013) 4601–4611.
[116] Z.Y. Hou, X.J. Li, C.X. Li, Y.L. Dai, P.A. Ma, X. Zhang, X.J. Kang, Z.Y. Cheng, J. Lin, Langmuir 29 (2013) 9473–9482.
[117] B.T. Song, C.T. Wu, J. Chang, Acta Biomater. 8 (2012) 1901–1907.
[118] L. Matlock-Colangelo, A.J. Baeumner, Lab Chip 12 (2012) 2612–2620.
[119] Z.G. Wang, L.S. Wan, Z.M. Liu, X.J. Huang, Z.K. Xu, J. Mol. Catal. B Enzym. 56 (2009) 189–195.
[120] G.L. Ren, X.H. Xu, Q. Liu, J. Cheng, X.Y. Yuan, L.L. Wu, Y.Z. Wan, React. Funct. Polym. 66 (2006) 1559–1564.
[121] M. Ahmad, C.F. Pan, Z.X. Luo, J. Zhu, J. Phys. Chem. C 114 (2010) 9308–9313.
[122] W. Wang, L.L. Zhang, S.F. Tong, X. Li, W.B. Song, Biosens. Bioelectron. 25 (2009) 708–714.
[123] Y. Ding, Y. Wang, L.A. Su, M. Bellagamba, H. Zhang, Y. Lei, Biosens. Bioelectron. 26 (2010) 542–548.
[124] D.P. Li, M.W. Frey, A.J. Baeumner, J. Membr. Sci. 279 (2006) 354–363.
[125] D.Y. Yang, X. Liu, Y. Jin, Y. Zhu, D.D. Zeng, X.Y. Jiang, H.W. Ma, Biomacromolecules 10 (2009) 3335–3340.
[126] P.H. Tsou, C.K. Chou, S.M. Saldana, M.C. Hung, J. Kameoka, Nanotechnology 19 (2008) 6.
[127] D.P. Wu, D.W. Han, A.J. Steckl, ACS Appl. Mater. Interfaces 2 (2010) 252–258.
[128] Y. Lee, H.J. Lee, K.J. Son, W.-G. Koh, J. Mater. Chem. 21 (2011) 4476–4483.
[129] D. Kai, M.P. Prabhakaran, B. Stahl, M. Eblenkamp, E. Wintermantel, S. Ramakrishna, Nanotechnology 23 (2012) 10.
[130] X.J. Loh, P. Peh, S. Liao, C. Sng, J. Li, J. Control. Release 143 (2010) 175–182.
[131] X.J. Loh, S.H. Goh, J. Li, Biomacromolecules 8 (2007) 585–593.
[132] X.J. Loh, Y.L. Wu, W.T.J. Seow, M.N.I. Norimzan, Z.X. Zhang, F. Xu, E.T. Kang, K.G. Neoh, J. Li, Polymer 49 (2008) 5084–5094.
[133] X.J. Loh, K.B.C. Sng, J. Li, Biomaterials 29 (2008) 3185–3194.
[134] X.J. Loh, Y.X. Tan, Z.Y. Li, L.S. Teo, S.H. Goh, J. Li, Biomaterials 29 (2008) 2164–2172.
[135] X.J. Loh, B.J.H. Yee, F.S. Chia, J. Biomed. Mater. Res. A 100A (2012) 2686–2694.
[136] X.J. Loh, W. Guerin, S.M. Guillaume, J. Mater. Chem. 22 (2012) 21249–21256.
[137] X.J. Loh, P.N.N. Vu, N.Y. Kuo, J. Li, J. Mater. Chem. 21 (2011) 2246–2254.
[138] X.J. Loh, J. Appl. Polym. Sci. 127 (2013) 2046–2056.